especially at the postgelation time. We summarize the main results and conclusions: (a) at least from the point of view of small (molecular) scale structural characteristics, the gelation point emerges as a relatively unspecial point, compared to the overall picture. (b) On a molecular scale, such as probed by Py, geometric complexity and irregularity start to build up mainly after the gelation point. Actually, in agreement with Schaefer et al.[11c] pH has only minor effect on this property at the early monomer–sol–gel stages. (c) Two general patterns of behavior were observed depending on w/s ratio. At low w/s ratio, geometric irregularity and porosity build up gradually along the whole process, resulting first in increase in Py emission intensity as Py aggregation becomes more pronounced, followed by decrease in intensity as Py molecules become isolated. At high w/s ratio, a smooth surface is formed, prior to the buildup of the porous structure. (d) From (c) we conclude that polymerization–gelation occurs at low w/s whereas formation of a colloid followed by its gelation occurs at high w/s. (e) Opposite effects of pH were observed, depending on w/s ratio. A relatively low degree of branching characterizes acidic pH at low w/s and basic pH at high w/s; A high degree of branching characterizes basic pH at low w/s and acidic pH at hig h w/s. (f) Ethoxy groups slow down the polymerization, in comparison with methoxy groups, but the reaction rates coincide, once all the alkoxy groups are hydrolyzed. (g) Once again,[4-6] the sol–gel process proved to be an efficient trap for isolation of organic molecules. The Py excimer disappears at the final xerogel stage. (h) The changes in the polarity of the Py environment along the sol–gel process, as reflected by the I_1/I_5 ratio, are not due to the support itself but to Py aggregation (conclusion c).

Elsewhere, we shall describe the use of other fluorescent probes, the polymerization of monoalkyltrialkoxysilane monomers, and structural dynamic oscillations at the gel–xerogel transition. For preliminary paper, see ref 5, 17.

Acknowledgment. This work is supported by the NCRD, Israel, and by the KFA, Julich, West Germany, and assisted by the F. Haber Research Center for Molecular Dynamics, Jerusalem. Helpful discussions with Professor M. Ottolenghi are gratefully acknowledged.

Registry No. $Si(OCH_3)_4$, 681-84-5; SiO_2, 7631-86-9; pyrene, 129-00-0.

Small-Angle Neutron Scattering from Water-in-Oil Microemulsions

E. Caponetti† and L. J. Magid

Department of Chemistry, University of Tennessee, Knoxville, Tennessee 37996-1600

J. B. Hayter

Solid State Division, Oak Ridge National Laboratory,‡ Oak Ridge, Tennessee 37831

J. S. Johnson, Jr.*§

Department of Chemistry, University of Tennessee, Knoxville, Tennessee 37996-1600, and Chemistry Division, Oak Ridge National Laboratory, Oak Ridge, Tennessee 37831

Received March 17, 1986. In Final Form: August 17, 1986

Small-angle neutron scattering (SANS) from water-in-oil microemulsions comprised of potassium oleate/hexadecane/water/1-pentanol or 1-hexanol is reported for several compositions and for different deuterated components. At all compositions (volume fraction of water ca. 0.11–0.29), strong scattering and peaks in intensities as a function of angle established structures in the solutions, characterized by distances of the order of 30 Å; these observations are contrary to inferences in the literature, based on indirect techniques. Of models tested, monodisperse oblate ellipsoids with a water core and a permeable shell gave reasonably satisfactory fits. Over the range of compositions covered, there appears to be no drastic change in structure nor any profound difference between 1-pentanol and 1-hexanol as cosurfactant.

Introduction

It is by now well-known that considerable quantities of water can be solubilized in hydrocarbons by surfactants, frequently assisted by alcohols. Conversely, hydrocarbons can be solubilized in water by such amphiphiles. These microemulsions are of considerable importance per se, for example, in certain types of catalysis. Motor fuel compositions incorporating water or alcohols distributed as microemulsions are being evaluated for enhanced fire and explosion safety, for lower emissions, and for possibilities of extension of petroleum with natural products. In addition, microemulsions dominate the chemistry underlying such processes as enhanced oil recovery by micellar floods. As the name implies, the minor component (aqueous or hydrocarbon) is distributed in a continuous phase of the major component in particles small compared to those of ordinary emulsions. At the extremes of composition, when the distribution is a relatively small amount of water in a large amount of oil (w/o; the case here) or vice versa

† Postdoctoral Fellow at the University of Tennessee, 1984. Permanent address: Istituto Fisica Chimica, University of Palermo, Palermo, Italy.

‡ Research sponsored by the U.S. Department of Energy under Contract DE-AC05-840R21400 with the Martin Marietta Energy Systems, Inc.

§ Research Professor, University of Tennessee, 1984. Consultant, Oak Ridge National Laboratory.

0743-7463/86/2402-0722$01.50/0

(o/w), there is general agreement about gross features. When water is the dominant component, hydrocarbon is distributed in the interior of surfactant micelles. In w/o systems, above certain concentrations sometimes in dispute, there are discrete aggregates with aqueous cores. There is less agreement about the intermediate range, in which extended water layers and oil layers separated by an amphiphile film ("bicontinuous structure"), as opposed to closed aggregates, have been proposed. In addition, there are open questions concerning details of structure of the closed aggregates and concerning whether it is more profitable to consider them as swollen micelles or as very fine dispersions, made possible by extremely low interfacial tensions. In the case of w/o dispersions of concern here, there have been proposals to distinguish reverse or inverted micellar compositions from microemulsion domains by, for example, the water-to-surfactant ratio at which the dimensions of the aggregates (of aerosol OT (AOT)/water in isooctane, as measured by dynamic light scattering in the example discussed) begin to vary with temperature.[1]

Peculiar aspects of the chemistry of w/o microemulsions imply that questions of more than nomenclature may be involved. Shah et al.[2,3] investigated as a function of added water several properties of a system comprised of 5 mL of hexadecane and 2 mL of hexanol per g of potassium oleate (KOl), approximately the same ratio of these components investigated here. At low water, a clear dispersion and a plateau in electrical conductivity were observed. There was then a turbid birefringent region, in which resistance dropped by 2 orders of magnitude and then traced a short plateau before going through a minimum; viscosities were high in this region. With further water addition, there was again a clear region, followed by an opaque dispersion. The turbid birefringent region was attributed to a transition of water-in-oil spheres to cylinders to lamellae and the clear region at higher water content to an oil-in-water dispersion. Systems of similar composition except for substitution[4] of 1-pentanol for 1-hexanol followed a similar pattern in appearance but had very different changes with water addition in NMR, electrical resistance, and viscosities. In the region from 0.1 to 0.6 volume ratio of water to oil, conductivity dropped by 4 orders of magnitude in the pentanol system, in contrast to essential constancy in hexanol, and the increase in viscosities was much greater in the hexanol system. Shah et al. concluded that amphiphiles and water were molecularly dispersed in the presence of pentanol.

Sjoblom and Friberg[5] identified by light-scattering subregions in the water-in-oil domain of potassium oleate systems containing pentanol (lower molecular weight hydrocarbons than those of Shah et al.) and concluded that inverse micelle formation began when the mole ratio of water to oleate exceeded 8. Bellocq and Fourche[6] reached a similar conclusion for the hexanol/dodecane pair. Boussaha et al.[7] interpreted positron annihilation rates as indicating that aggregation occurs above a 0.4 water/oil volume ratio in the presence of pentanol; they concluded that the transition from solubilization to inverse micelles occurred at a 0.2 ratio in the presence of hexanol (the hydrocarbon was hexadecane). Atik and Thomas[8] found differences in quenching by potassium ferricyanide of fluorescence in hexanol- and pentanol-containing microemulsions. Their results for the pentanol system with the same components Shah used could have been interpreted to indicate a molecularly dispersed system. However, on the basis of other measurements in which the hydrocarbon was dodecane rather than hexadecane and in which the pentanol-to-surfactant ratio was varied to give a single phase, they concluded that water pools exist under all conditions they investigated; with hexadecane, their water/oil volume ratio appears to have been >0.2 in all cases. The differences in quenching kinetics were attributed to a much more rapid exchange of quencher between water pools when the alcohol was pentanol, rather than hexanol. Our results from the more direct SANS method will clearly show the existence of structures in compositions at which some of these authors concluded only molecular dispersions existed.

Boned et al.[9] measured conductivity and permittivity over several compositional paths of the w/o region of this system with hexanol, the surfactant/alcohol ratio being the same as used by Shah et al. From minima and inflections in these scans, they divided the apparently isotropic region into three subregions: (1) at low water/oleate ratio, a dispersion of hydrated soap aggregates; (2) at intermediate ratios, inverse micelles; and (3) at high water/soap, coalesced or clustering micelles. They state that conductivity behavior as a function of water content with hexanol as cosurfactant cannot be explained by percolation theory, in contrast to Shah's results with pentanol-containing systems.

The differences in properties of visually clear microemulsions arising from a difference of one carbon in the alcohol is interesting, as are the sources of the major changes in properties with water content. Small-angle neutron scattering (SANS) can provide information on structural changes accompanying these differences. The size of the aggregates should be in the range accessible to the technique and the differences in scattering by hydrogen and deuterium allow inferences concerning the location of protiated and deuterated components. SANS has been applied to a number of w/o microemulsions. For example, the water/cyclohexane/sodium dodecyl sulfate/1-pentanol system was investigated with D_2O, with C_6D_{12}, and with D_2O and various ratios of C_6H_{12} to C_6D_{12}.[10-12] The volume ratios were low enough in some cases[10] for the effect of interparticle structural factors on scattering to be small, and interpretation was feasible in terms of Guinier radii.[13] Values of the radius of the water core and of R_G for the overall particle (affected by penetration of hydrocarbon in the shell) were consistent with results of ultracentrifugation. At high water fractions,[11] onset of polydispersity and inversion to an o/w system was inferred. Ober and Taupin[14] determined osmotic compressibilities by extrapolation of scattering intensity curves to zero angle and inferred hard-sphere radii of the particles. They found that attraction was too strong to be explained by van der Waals potentials, a conclusion earlier reached by Agterof

(1) Zulauf, M.; Eicke, J. F. *J. Am. Chem. Soc.* **1979**, *83*, 480.
(2) Shah, D. O.; Hamlin, R. M. *Science (Washington, D.C.)* **1971**, *171*, 483.
(3) Falco, J. W.; Walker, R. D.; Shah, D. O. *AICHE J.* **1974**, *20*, 510.
(4) Shah, D. O.; Bansal, V. K.; Hsieh, W. C. In *Improved Oil Recovery by Surfactant and Polymer Flooding*; Academic Press: New York, 1977; p 293.
(5) Sjoblom, E.; Friberg, S. *J. Colloid Interface Sci.* **1978**, *67*, 16.
(6) Bellocq, A. M.; Fourche, G. *J. Colloid Interface Sci.* **1980**, *78*, 275.
(7) Boussaha, A.; Djermouni, B.; Fucugauchi, L. A.; Ache, H. J. *J. Am. Chem. Soc.* **1980**, *102*, 4654.
(8) Atik, S. S.; Thomas, J. K. *J. Phys. Chem.* **1981**, *85*, 3921.
(9) Boned, C.; Clausse, M.; Lagourette, B.; Peyrelasse, J.; McClean, V. E. R.; Sheppard, R. J. *J. Phys. Chem.* **1980**, *84*, 1520.
(10) Dvolaitzky, M.; Guyot, M.; Lagues, M.; LePesant, J. P.; Ober, R.; Sauterey, C.; Taupin, C. *J. Chem. Phys.* **1978**, *69*, 3279.
(11) Lagues, M.; Ober, R.; Taupin, C. *J. Phys. (Lett.)* **1978**, *39*, L-487.
(12) Dvolaitzky, M.; Lagues, M.; LePesant, J. P.; Ober, R.; Sauterey, C.; Taupin, C. *J. Phys. Chem.* **1980**, *84*, 1532.
(13) Guinier, A.; Fournet, G. *Small Angle Scattering of X-Rays*; Wiley: New York, 1955; pp 24–28.
(14) Ober, R.; Taupin, C. *J. Phys. Chem.* **1980**, *84*, 2418.

et al.[15] from light scattering of w/o microemulsions. For systems without added salt, Ober and Taupin found it necessary to postulate prolate ellipsoids to fit their results.

Auvray et al.[16] and de Geyer and Tabony,[17] on the basis of SANS from microemulsions in two- and three-phase regions of water/toluene/sodium dodecyl sulfate/1-butanol systems, claim evidence for domains where bicontinuous or intercontiguous structures exist.

Cabos and Delord[18] investigated a ternary w/o system, water/AOT/*n*-heptane. The solutions were dilute enough for the results not to be affected seriously by interparticle interactions. Surfactant molecules per aggregate estimated from variation of contrast, C_7H_{16}/C_7D_{16} and H_2O/D_2O, agreed well; aggregation numbers increased sharply with the ratio of water/AOT. Robinson and co-workers have also made measurements on the water/AOT/*n*-alkane systems.[19-21]

With respect to interpretation of experimental results, two investigations are more pertinent to the approach used here than those previously cited. Cebula et al.[22] applied several techniques to the system sodium dodecylbenzenesulfonate/xylene/water/hexanol, the SANS measurements covering a volume fraction of water from about 0.15 to 0.5. At these concentrations, interparticle interactions are expected to be important, and this was evidenced by peaks in the scattering intensity as a function of angle, expressed as Q ($= (4\pi/\lambda) \sin \theta$, where λ is the wavelength of the neutrons and 2θ is the scattering angle). In the fit to the results they used a hard-sphere structure factor[24] and a model involving a water core plus a shell of somewhat different scattering density than the xylene continuous phase. The varied parameter was the radius of the core, the hard-shell radius being taken to be this value plus a constant thickness. Computations were carried out for various values of thickness, scattering density of the shell, and a standard deviation of size for a polydisperse distribution. They were able to reproduce the features of the curves with plausible values of these parameters. The shell thickness was less than one would compute from the total stoichiometric particle less the water core, an indication of interpenetration of surfactant hydrocarbon in the closest approach of the particles. The value of shell thickness was approximately the length of the alcohol. Similar inferences were drawn from scattering by systems comprised of potassium oleate/toluene/water/hexanol[23a] and potassium oleate/dodecane/water/hexanol.[23b]

Huang et al.[25] also carried to high volume fractions measurements of AOT micelles in deuterated octane and to a moderate concentration measurements of an AOT/D_2O microemulsion in decane. They also used a hard-sphere model to calculate structure factors but added a perturbation from a short-range square-well attractive potential.[26]

We have mentioned several interesting questions posed by results in the literature concerning the specific w/o systems of interest in this paper. Their resolution would shed light on more general aspects of the class, such as how much water is necessary for formation of inverse micelles.[27] The literature cited covers ranges of compositions much wider than we have covered so far by SANS. We have elected to concentrate on high volume fractions of disperse phases in the time so far available to us on the spectrometer, because the most interesting open questions seem to us to be in these regions. One disadvantage of this choice is the fact that methods of data analysis are not as highly developed as for more dilute systems. Although there are details of interest we are not yet able to delineate, we can from present results definitively identify the occurrence of sizeable structures in the solutions and can estimate with reasonable confidence the dimensions characterizing them.

Table I. Microemulsion Compositions

	KOl	*N*-hexadecane	1-pentanol	1-hexanol	D_2O	vol. fraction[a]
A	1 g	5 mL	2 mL		1 mL	0.41
mol	1	5.54	5.96		17.8	
B	1 g	5 mL	2 mL		2.5 mL	0.52
mol	1	5.52	5.97		44.6	
C	1 g	5 mL		2 mL	2.5 mL	0.52
mol	1	5.54		5.18	44.6	
D	1 g	5 mL	2 mL		3.27 mL	0.56
mol	1	5.52	5.97		57.0	
E(CHD)	1 g	4.42 mL	1.99 mL		2.55 mL	0.55
mol	1	4.85	5.89		45.3	
		$C_{16}D_{34}$				
F(CDH)	1 g	4.42 mL	2.02 mL		2.49 mL[b]	0.55
mol	1	4.84	5.99		44.2	
G(CDD)	1 g	4.36 mL	2.06 mL		2.51 mL	0.56
mol	1	4.79	6.11		44.4	

[a] Surfactant + alcohol + D_2O (or H_2O). [b] H_2O.

Experimental Section

Materials. Scattering measurements were carried out on three compositions, in which D_2O was the only deuterated component, with 1-pentanol as cosurfactant and with different amounts of D_2O and on one composition with 1-hexanol as cosurfactant. Another set of three solutions were of approximately the same molar concentration but were made up with D_2O or $C_{16}D_{34}$ or both, pentanol being the alcohol. Compositions are given in Table I; the volume fractions listed are upper limits of the disperse phase, because some of the alcohol is probably distributed in the hexadecane, rather than the particles. The deuterated hexadecane was obtained from Cambridge Isotopes Laboratories and was stated to be of 96% isotopic purity. In the analysis of results, allowance was made for the 4% proton content.

SANS Measurements. Neutron scattering measurements were performed on the 30-m (source to detector) instrument of the National Center for Small-Angle Scattering Research (NCSASR) located at the High Flux Isotope Reactor, Oak Ridge National Laboratory. Samples A–D of Table I were contained in cylindrical quartz spectrophotometric cells of 2-mm path length and E–G in 1-mm cells, which were thermostated at 25 ± 0.05 °C by means of circulation from an external bath. Correction for detector background and sensitivity and for scattering by the empty cell and conversion of patterns to radial averages were by programs provided by the Center, as earlier.[28] These programs

(15) Agterof, W. G. M.; Van Zomeren, J. A. J.; Vrij, A. *Chem. Phys. Lett.* **1976**, *43*, 363.
(16) Auvray, L.; Cotton, J.-P.; Ober, R.; Taupin, C. *J. Phys. Chem.* **1984**, *88*, 4586.
(17) de Geyer, A.; Tabony, J. *Chem. Phys. Lett.* **1985**, *113*, 85.
(18) Cabos, C.; Delord, P. *J. Appl. Crystallogr.* **1979**, *12*, 502.
(19) Fletcher, P. D. I.; Howe, A. M.; Perrins, N. M.; Robinson, B. H.; Toprakcioglu, C.; Dore, J. C. In *Surfactants in Solution*; Mittal, K., Lindman, B., Eds.; Plenum Press: New York, 1984; Vol. 3, p 1745.
(20) Robinson, B. H.; Toprakcioglu, C.; Dore, J. C. *J. Chem. Soc., Faraday Trans. 1* **1984**, *80*, 13.
(21) Toprakcioglu, C.; Dore, J. C.; Robinson, B. H.; Howe, A. *J. Chem. Soc., Faraday Trans. 1* **1984**, *80*, 413.
(22) Cebula, D. J.; Ottewill, R. H.; Ralston, J.; Pusey, P. N. *J. Chem. Soc., Faraday Trans. 1* **1981**, *77*, 2585.
(23) (a) Cebula, D. J.; Harding, L.; Ottewill, R. H.; Pusey, P. N. *Colloid Polym. Sci.* **1980**, *258*, 973. (b) Cebula, D. J.; Myers, D. Y.; Ottewill, R. H. *Colloid Polm. Sci.* **1982**, *260*, 96.
(24) Ashcroft, N. W.; Lekner, J. *Phys. Rev.* **1966**, *145*, 83.
(25) Huang, J. S.; Safran, S. A.; Kim, M. W.; Grest, G. S.; Kotlarchyk, M.; Quirke, N. *Phys. Rev. Lett.* **1984**, *53*, 592.
(26) Sharma, P. V.; Sharma, K. C. *Physica A (Amsterdam)* **1977**, *89A*, 213.
(27) Eicke, H. P.; Christen, J. *Helv. Chim. Acta* **1978**, *61*, 2258.

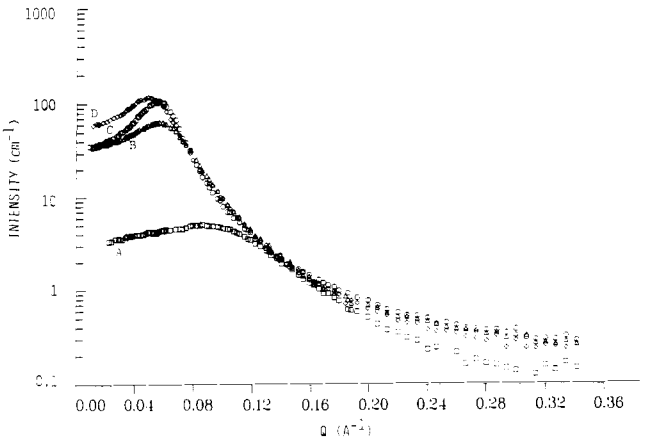

	KOl, mol	n-$C_{16}H_{34}$, mol	1-pentanol, mol	1-hexanol, mol	D_2O, mol	ϕ_v
A	1	5.5	6.0		18	0.41
B	1	5.5	6.0		45	0.52
C	1	5.5		5.2	45	0.52
D	1	5.5	6.0		57	0.55

Figure 1. Scattering from D_2O-in-oil microemulsions.

also compute statistical errors for these averages. Scattering cross sections, $d\Sigma/d\Omega$ (cm^{-1}) = $I(Q)$, were obtained from these averages by factors also provided by the Center, determined from scattering of substances of known cross section or by calibrations with H_2O or Al-4, a porous sample provided by the Center as a secondary standard. In view of the high fraction of "solute" components, the usual subtraction of scattering by pure solvent seemed questionable. For samples A–D, we subtracted instead a pattern from an H_2O/D_2O solution of a ratio selected to have the same incoherent scattering length density as the solution. A similar difference pattern could be obtained by subtracting intensities from hexadecane multiplied by fraction of hexadecane in the solution. Residual incoherent scattering was accounted for by a parameter (B) in the least-squares fit making a contribution to intensity invariant with Q. Results for sample-to-detector distances of 1.4, 2.4, and 8.1 m are reported, the range of Q being ~0.01–0.35 $Å^{-1}$. For samples E–G, only corrections for detector background and empty cell were made, and incoherent scattering was accounted for by least-squares parameter B. In these cases, samples-to-detector distances at the High Flux Isotope Reactor were 12, 4, and 1.4 m, the Q-range being approximately the same. We combined with this set measurements at 4.6 meters obtained at the Center's SANS system at the Oak Ridge Research Reactor. Agreement between the measurements with the two systems was good. Runs at the different distances were combined by programs provided by the Center.

Results and Discussion

Combined patterns for compositions A–D are presented in Figure 1 and for E–G, in which scattering contrast was varied by use of different deuterated components for essentially the same molar concentrations, in Figure 2. The intense patterns obtained in all cases establishes unequivocally that aggregates are present. The minimum dimension within an aggregate may be estimated from the decay of intensity in reciprocal space, without regard to model. In Figure 1, this gives a dimension of the order of $\pi/0.1$, or 30 Å, in contradiction to inferences from other techniques in some of the references cited that solutes are molecularly dispersed at some of the stoichiometries investigated. The peaks in intensity indicate local order over a range several times that corresponding to molecular dimensions. These inferences rely only on the rigorous Fourier integral theorem and are independent of any model

(28) Triolo, R.; Magid, L. J.; Johnson, J. S., Jr.; Child, H. R. *J. Phys. Chem.* **1983**, *86*, 2389.

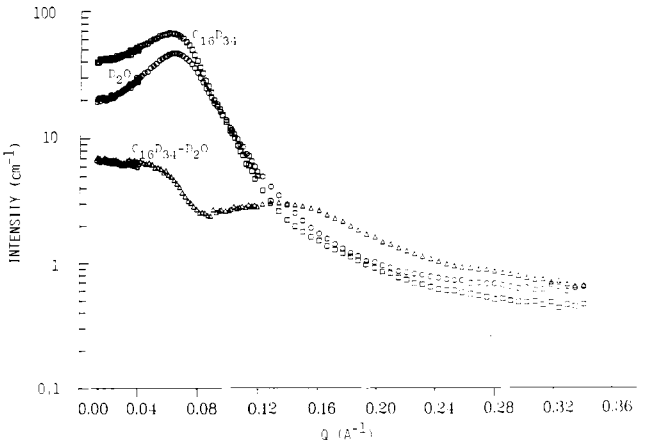

Figure 2. Scattering from water-in-oil microemulsions; different contrasts. Approximate mol/mol of potassium oleate: hexadecane, 4.8; 1-pentanol, 6; water, 45.

of the microemulsion. In extending our interpretation, there are two extreme models that could be used: a fluid containing discrete aggregates and a bicontinuous structure. Absence of oscillations or sharp peaks in the patterns argue that there is no very long-range order, and if there is a bicontinuous arrangement, it must be irregular or transient.

When the scattering-length densities of water and of oil are approximately matched (see Figure 2, $C_{16}D_{34}/D_2O$), scattering is still observed; further, there is a broad peak at intermediate Q. Only the hydrocarbon of the surfactant and cosurfactant provide appreciable contrast in this case, and the fact that there is a pattern shows that they must form a correlated structure, although nothing can be inferred about symmetry because of angle averaging. The observations are consistent with scattering from a surfactant/cosurfactant shell between water droplets and a continuous oil phase, if the aggregates present are closed. A transient bicontinuous phase, in which the water droplets fluctuate and may coalesce for short times, would look similar when averaged over the time scale of a SANS experiment and would provide a path for electrical conduction at the water volume fraction here, with resistance dependent on the frequency of the fluctuations.

The two extreme models posed are therefore locally similar. Consequently, we can approximate the local geometry around aqueous regions by using simple water-droplet-in-oil models, for which we can calculate scattering patterns at various levels of approximation. The results should not, however, be taken to indicate that the transient alternative necessarily does not exist. Dense fluids such as these will in any case have significant local-neighbor order.

Analysis of Scattering Patterns. Several models were tested for success in least-squares fitting in reproducing the scattering patterns. All postulated a water core, with inclusion of the carboxylate head groups and potassium counterions of the oleate and OH group of the alcohol. All of the surfactant was assigned to the aggregates, and approximately half of the stoichiometric alcohols per oleate (3 for A–B and D–G and 2.5 for C) were arbitrarily also put in the aggregates; test of other plausible alcohol distributions indicated little effect on fits or parameters at least when D_2O was the only deuterated component. The core is surrounded by a shell made up of the hydrocarbon parts of the surfactant and alcohol in the initial model. In the simplest model, monodisperse spheres, the intensities are given by

$$I(Q) = N_P S(Q) P(Q) + B \quad (1)$$

Table II. Volumes of Groups (Å³)

$-CH_3$	54.3	K^+	6.6
$-CH_2-$	26.9	D_2O or H_2O	30.0
$-CH=$	20.6	$-OH$	17.0
$-COO^-$	25.4		

where N_P is the number of particles/centimeter cubed, $S(Q)$ is the structural function arising from interparticle scattering, $P(Q)$ is the particle scattering function, and B is the constant contribution of residual incoherent scattering. A hard-sphere structural function[24] was used initially. This was computed with the program of Hayter and Penfold,[29] either in the limiting case of vanishingly small external potential or with a small surface attraction. The particle scattering function is given by

$$P(Q) = (4\pi/3)^2(R_1^3(\rho_1 - \rho_2)F_0(QR_1) + R_2^3(\rho_2 - \rho_s)F_0(QR_2))^2 \quad (1A)$$

R_1 being the radius of the core (Å), ρ_1 the scattering length density of the core (cm/Å³), subscript 2 indicating the same quantities for the shell, and $F_0(x) = 3(\sin x - x \cos x)/x^3$. Subscript s denotes the solvent, here hexadecane plus alcohol not included in the aggregates. Scattering lengths for the atoms comprising the various constituents were obtained from standard compilations, e.g., ref 30, and volumes for various groups from the literature.[31-33] The volumes used are summarized in Table II.

It will be seen that adequate fits were not obtained by postulation of monodisperse spheres, for which computations gave oscillations in intensity with Q not seen in the results. Anisotropy or polydispersity would be expected to damp such oscillations. For departure from sphericity, monodisperse prolate and oblate ellipsoids were tested. Here eq 1 is replaced by[34b,35]

$$I(Q) = N_p[\langle|F(\vec{Q})|^2\rangle + |\langle F(\vec{Q})\rangle|^2(S(Q) - 1)] + B \quad (2)$$

The ellipsoids are described by three dimensions, conventionally selected as semiaxes, two (l) the same and the third, el; the volume $v = (4\pi/3)l^3e$, the axial ratio e being greater than one for prolate and less than one for oblate. The scattering of asymmetric particles must take into account all orientations with repsect to the neutron beam, thus

$$\langle|F(\vec{Q})|^2\rangle = \int_0^1 |F(\mathrm{ELL})|^2 \, d\mu \quad (3a)$$

$$|\langle F(\vec{Q})\rangle|^2 = |\int_0^1 F(\mathrm{ELL}) \, d\mu|^2 \quad (3b)$$

μ being the cosine of the angle of the direction of the long dimension, and for the core (1) and shell (2) case here

$$F(\mathrm{ELL}) = v_1(\rho_1 - \rho_2)F_0(u_1) + v_2(\rho_2 - \rho_s)F_0(u_2) \quad (4)$$

where $u_i = Q[e_i^2l_i^2 + l_i^2(1 - \mu^2)]^{0.5}$, v_2 being the volume of the overall aggregate. The integrals 3a and 3b are evaluated numerically.

Fits to a polydisperse distribution of spheres were also tested. We used a Schulz distribution

$$f(R) = (Z + 1)^{Z+1}X^Z \exp[-(Z + 1)\, X]/R\Gamma(Z + 1)$$

X being $R/\bar{R}$, with $\bar{R}$ the mean radius. This distribution is characterized by a breadth parameter, $Z = (1 - (\sigma/\bar{R})^2)/(\sigma/\bar{R})^2$, where σ is the variance and Γ represents the Γ function. Equations for intensity are similar in form to those of ellipsoids, with the replacement of (3a) and (3b) with

$$\langle|F(Q)|^2\rangle = \int |F(Q,R)|^2 f(R) \, dR \quad (5a)$$

$$|\langle F(Q)\rangle|^2 = |\int F(Q,R) f(R) \, dR|^2 \quad (5b)$$

The $F(Q,R)$ for each size of particle is the square root of $P(Q)$ in eq 1A. Analytical expressions for computations with this distribution are available.[34b,35]

In both the asymmetric particle and the polydisperse sphere case, the structural factor we shall use is that computed[29] for a sphere of size equivalent to the ellipsoid or the (weight) average particle size. This is of course an approximation and, for polydisperse hard-sphere systems, not a very good one.[36] Chen et al.[37] concluded that a better approximation for polydisperse systems under some conditions may be given by replacing $P(Q)$ in eq 1 by $\langle|F(Q)|^2\rangle$.

Zero-angle intensity is fixed by the particle concentration, N_P, the contrasts and dimensions of the various regions of the particles, and the structural function at zero angle, which is directly related to the free-energy gradients with concentration of particles or osmotic compressibility. The particle dimensions selected by the least-squares fit, constrained by stoichiometry, determine the value of N_P. Absolute intensities are therefore derived from the fit. However, these values are experimentally less precise than relative intensities as a function of angle. NCSASR estimates that the calibration standards and procedures are good to ~10% in absolute intensity. In addition, residual errors in the correction for differences in coherent scattering between sample and background[38] and errors in transmission measurements add to uncertainties in normalization of intensities to absolute values. To avoid distortions of other parameters to compensate for errors in absolute intensity, we include an adjustable parameter A ("scale") multiplied by the terms in equations for intensity involving $S(Q)$ and $P(Q)$. If there are no errors from these sources, its value should be 1, but if A is within ~15% of unity, we do not infer problems with the model under test. This point is discussed further in ref 34b.

The fits to experiment were by weighted nonlinear least squares. The weights of the intensities used were the reciprocal of their variances, v. Choice between models was primarily from visual agreement between experimental and computed intensities, along with the reasonableness of converged parameters. For rough comparison of fits, we also report a number derived from the weighted sum of residuals,

$$\mathrm{AVD} = [\Sigma_i[(\mathrm{obsd}_i - \mathrm{calcd}_i)^2/v_i]/(\mathrm{NPT} - \mathrm{NPAR} + 1)]^{1/2}$$

NPT being the number of observations and NPAR the number of varied parameters.

The evolution of models was an iterative procedure, unnecessary to follow in detail. We shall illustrate, however, improvement in fits attained with increasing elaboration. We first discuss the effect of structure-function

(29) Hayter, J. B.; Penfold, J. *Mol. Phys.* **1981**, *42*, 109; *J. Chem. Soc., Faraday Trans. 1* **1981**, *77*, 1851.
(30) Kostorz, G.; Lovesey, S. W. *Treatise on Materials Science and Technology*; Academic Press: New York, 1979; Vol. 15, pp 230–231.
(31) Tanford, C. *The Hydrotropic Effect: Formation of Micelles and Biological Membranes*; Wiley: New York, 1973.
(32) Immirzi, A.; Perini, B. *Acta Crystallogr., Sect. A* **1972**, *33*, 216.
(33) Millero, F. J. In *Water and Aqueous Solutions*; Horne, R. A., Ed.; Wiley-Interscience: New York, 1972; Chapter 13, p 519.
(34) (a) Hayter, J. B.; Penfold, J. *Colloid Polym. Sci.* **1983**, *261*, 1022. (b) Hayter, J. B. In *Physics of Amphiphiles: Micelles, Vesicles and Microemulsions*; DeGiorgio, V., Corti, M., Eds.; North Holland: Amsterdam, 1985; p 59.
(35) Kotlarchyk, M.; Chen, S.-H. *J. Chem. Phys.* **1983**, *79*, 2461.
(36) van Beurten, P.; Vrij, A. *J. Chem. Phys.* **1981**, *74*, 2744.
(37) Chen, S.-H.; Lin, T. L.; Kotlarchyk, M., paper to be published in the Proceedings, 5th International Symposium on Surfactants in Solutions, Bordeaux, July, 1984.
(38) Akcasu, A. Z.; Summerfield, G. C.; Jahshan, S. N.; Han, C. C.; Kim, C. Y.; Yu, H. *J. Polym. Sci., Polym. Phys. Ed.* **1980**, *18*, 863.

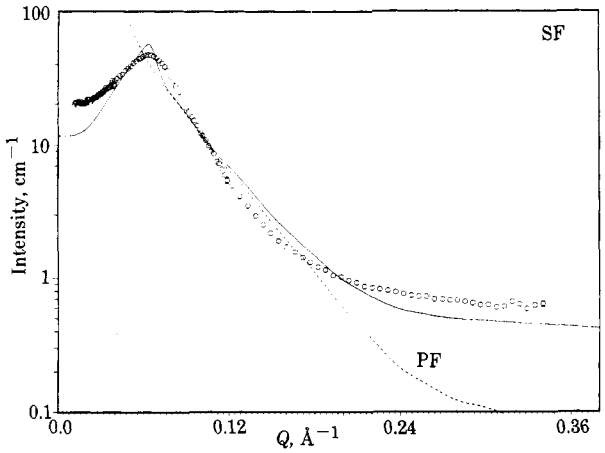

Figure 3. Fit to SANS pattern, composition E. Monodisperse ellipsoids, no penetration. Varied parameters: R_{core} = 43 ● 0.3; AR = 0.20 ± 0.01; scale = 1.22 ± 0.02; incoherent = 0.37 ± 0.08; AVD, 31.

parameters with a model we have found to give the most satisfactory fits, oblate ellipsoids. We use a composition in which D_2O provides most of the contrast, because of the relative simplicity of $P(Q)$. In fact, in these cases, as one might expect, inconsequential differences were found when the scattering-length density of the shell was assigned the same value as that of the continuous phase, rather than computing it separately ("invisible shell" model).

Structural Function Parameters. Two parameters are important in computation of structural functions for uncharged systems such as those of interest here: a radius, commonly referred to as "hard sphere", here designated as R_{sf} for structural factor, describing the closest approach of particles to one another, and the volume fraction, η, of the disperse phase, the fraction of volume occupied by the particles.

Figure 3 gives the fit for a basic model: varied (in addition to the scale factor A and incoherent factor B) are the radius of the aqueous core, R_{core} (comprised of water, surfactant head groups, counterions, and OH groups of the alcohols assigned to the particle), and the axial ratio of the ellipsoid, which yield η and R_{sf} as follows. The core radius is that of a sphere of volume equivalent to the volume of the ellipsoidal core. From it and the stoichiometry, the number of surfactant molecules/particle, AGG, is obtained. The alcohols were partitioned 1:1 between particles and solvent, here 3 mol per mol of potassium oleate assigned to the particle; in D_2O-only systems, varying this number had only minor effects on the fits. The volume of the total particle was computed by adding to the core volume the volume of the hydrocarbon parts of the surfactant and particle alcohols. From this volume, the equivalent-sphere radius of the total particle, R_{tot}, was computed, and this value was used as R_{sf}. In computing the particle function, the scattering-length density of the shell was taken to be the same as that of the continuous phase, comprised of hexadecane and the rest of the alcohol. Volume fraction etc. of the disperse phase was computed from the volume of water, surfactant, and particle alcohol. Figure 3 shows that this model, although qualitatively correct, is quantitatively inadequate. The particle function (PF) and structure function (SF) are sketched in the figure; these are not to scale, SF approaching unity at the right side of the graph. We must now identify which aspects of this apparently realistic model require improvement.

It seemed possible that effects on the structure function of the penetration of the shell by solvent hydrocarbon or by the shells of other particles might not be accounted for by this model. Analyses in the literature[34b,39] suggest that allowance can be made for such "permeability" by multiplying the volume fraction by a factor varying from one for no penetration, in which case R_{sf} would truly be a hard-sphere radius, to zero for the case of complete penetration. The permeable sphere theory is not strictly applicable, because it implies the densities in the interpenetrating regions are the sum of the components, but it should give a better approximation for interpenetrating shells.

Figure 4 shows the effect of varying a penetration factor, multiplied by the disperse-phase volume fraction (I) and computing R_{sf} as for Figure 3; of setting the penetration factor at unity and varying R_{sf} (II); and of varying both (III). The AVD values confirm the visual impression that (III) is the best fit. Also persuasive are the values of the parameters. With no penetration allowed, the core radius is larger than R_{sf}, a physically unreasonable dimension. Attempts to duplicate the effects of interpenetration by including an attractive interparticle potential give a much less adequate representation of the data. The fits to be presented therefore include no attractive potential.

Geometry of Micelles. The previously mentioned observation that our best fits have been obtained by monodisperse ellipsoid models holds for all compositions. We illustrate it here by a comparison of the other three geometries tested in Figure 5, again with composition E. The structure factor parameters were obtained as in Figure 4. Monodisperse spheres (I) fail most clearly to represent observations of the three, but the computed curves for polydisperse spheres (II) and monodisperse prolate ellipsoids (III) are also less like the experimental intensities than for monodisperse oblate ellipsoids (Figure 4, III). The AVD values of the fits in Figure 5 are also substantially higher than for the monodisperse ellipsoid and the uncertainties of the parameter values greater. The values of core radii are not tremendously different for the four geometries (the value listed for the polydisperse case is based on a number average and would be 25.5 on a weight-average basis for the Schulz parameter obtained in the fit).

It is interesting to note that in this concentrated system we are able to obtain much better fits from the ellipsoid model than from a model of polydisperse spheres, since in a dilute system, it is well-known that such a distinction cannot be made in practice.[34b] The underlying reason may be seen by considering the low-Q limit of eq 2, in which $F(Q)$ becomes independent of orientation as $Q \rightarrow 0$. In the case of monodisperse ellipsoids, no further averaging remains and $\langle|F(0)|^2\rangle = |\langle F(0)\rangle|^2$, whereas these size-averaged quantities differ in the case of polydisperse spheres, becoming respectively the sixth moment and the square of the third moment of the size distribution. The latter are easily distinguished using absolute intensity, unless the size distribution is very narrow.

Contrast. Varying the visibility to neutrons of different regions of the aggregates can be expected to illuminate further aspects of their structure. It is clear in such a case that an invisible shell model is not appropriate, and the fits to be presented of the systems E–G having different components deuterated are carried out with a core + shell model. For computation of the particle scattering function, R_{tot} (and the shell thickness and scattering length density consistent with R_{tot}) is computed by assigning to the shell the hydrocarbon parts of the surfactant and micelle cosurfactant; the value of AGG is obtained as before from the least-squares-derived core radius (the same result is

(39) Blum, L.; Stell, G. *J. Chem. Phys.* **1979**, *71*, 42; **1980**, *72*, 2212.

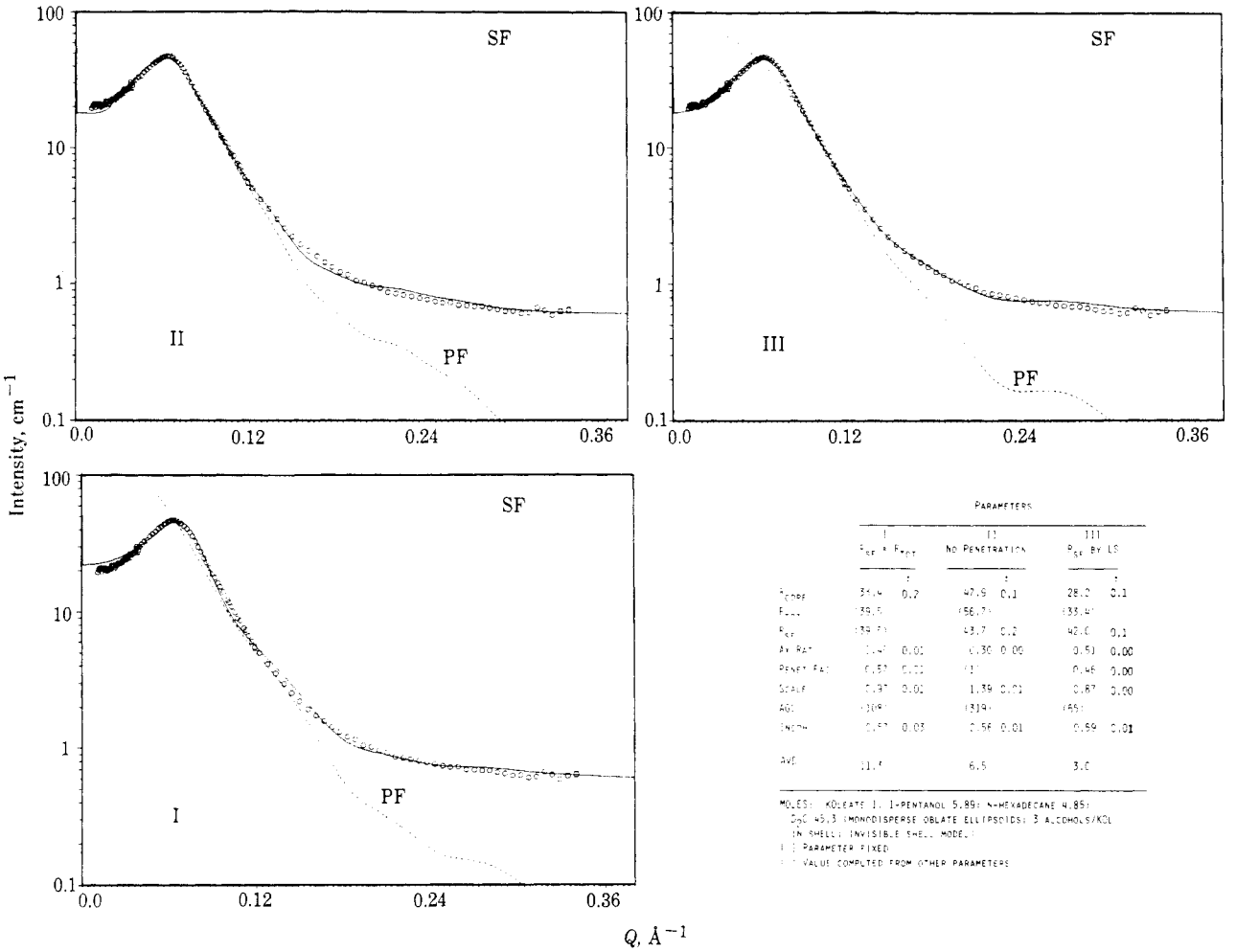

Figure 4. Structure function parameters; invisible shell model. Composition E.

obtained, as expected, from varying R_{tot} to determine AGG and deducing R_{core}). The radius for the structure function, R_{sf}, is varied independently. With deuterated continuous phase, there is a logical discrepancy in the independent variation of R_{sf}, in that solvent penetration should affect the scattering length density of the shell. The effect will be compensated to some extent in that lowering of intensity because of lower shell–solvent contrast will be counteracted by increased scattering because of greater shell thickness.

This model gave an essentially identical fit and the same parameters as the invisible shell for E, which has only water deuterated (Figures 4, III, and 6, I). The scattering-length densities for the core + shell fit were 3.55×10^{-7} Å^{-2} for the shell and -3.11×10^{-7} Å^{-2} for the continuous phase, in comparison with 6.01×10^{-6} Å^{-2} for the core.

The fit to the case of deuterated hexadecane (Figure 6, II), in which dominant contrast is between the total aggregate and the continuous medium, is good, though not so good as for D_2O. The magnitudes of the parameters in the two fits are very close. Their agreement increases confidence in the basic features of the model.

The fit (Figure 6, III) to the case in which there is strong contrast between the shell and both the core and medium reproduces only general aspects of the results, and the parameters, particularly the absolute scale, vary considerably from those derived from the patterns of solutions E and F. (Some of the discrepancy may arise from instrumental smearing, to which this case would be particularly vulnerable.) It seems likely that details of structure to which the other contrasts are indifferent may be important here. In solutions E and F, there is strong contrast between relatively extensive regions in the particle and the medium. The lower overall intensity level of G may accentuate the effect of penetration of the shell by hydrocarbon from solvent or other particles.

We have tried a model in which the core radius and the shell thickness was varied (in addition to axial ratio, penetration factor, and the scale and incoherent parameters). The shell was comprised of surfactant hydrocarbon, hydrocarbon of the 1-pentanol assigned to the particles, and enough hydrocarbon from the continuous phase or other particles to fill the shell volume. The scattering-length density of the invading hydrocarbon was taken to be the average of surfactant and of continuous-phase hydrocarbon, weighted by stoichiometry. Here R_{sf} was computed as the equivalent sphere radius corresponding to the total volume of the particle, rather than evaluated as an independently varied parameter. In this case, the number of alcohols assigned to the particle had a noticeable effect; between 4 and 6 mol of pentanol/potassium oleate gave reasonable results.

The fit and parameters allowing alcohols per potassium oleate to vary are given in Figure 7. Although details of the model appear to be washed out in the observed values, the fit is considerably closer than in Figure 6 (III), the AVD being cut almost in half. The parameters are considerably closer to those obtained for the same compositions with different contrast than those listed in Figure 6.

Other Compositions. Monodisperse oblate ellipsoids give reasonable fits to the other compositions reported, all having only water deuterated (Figure 8, parameters in

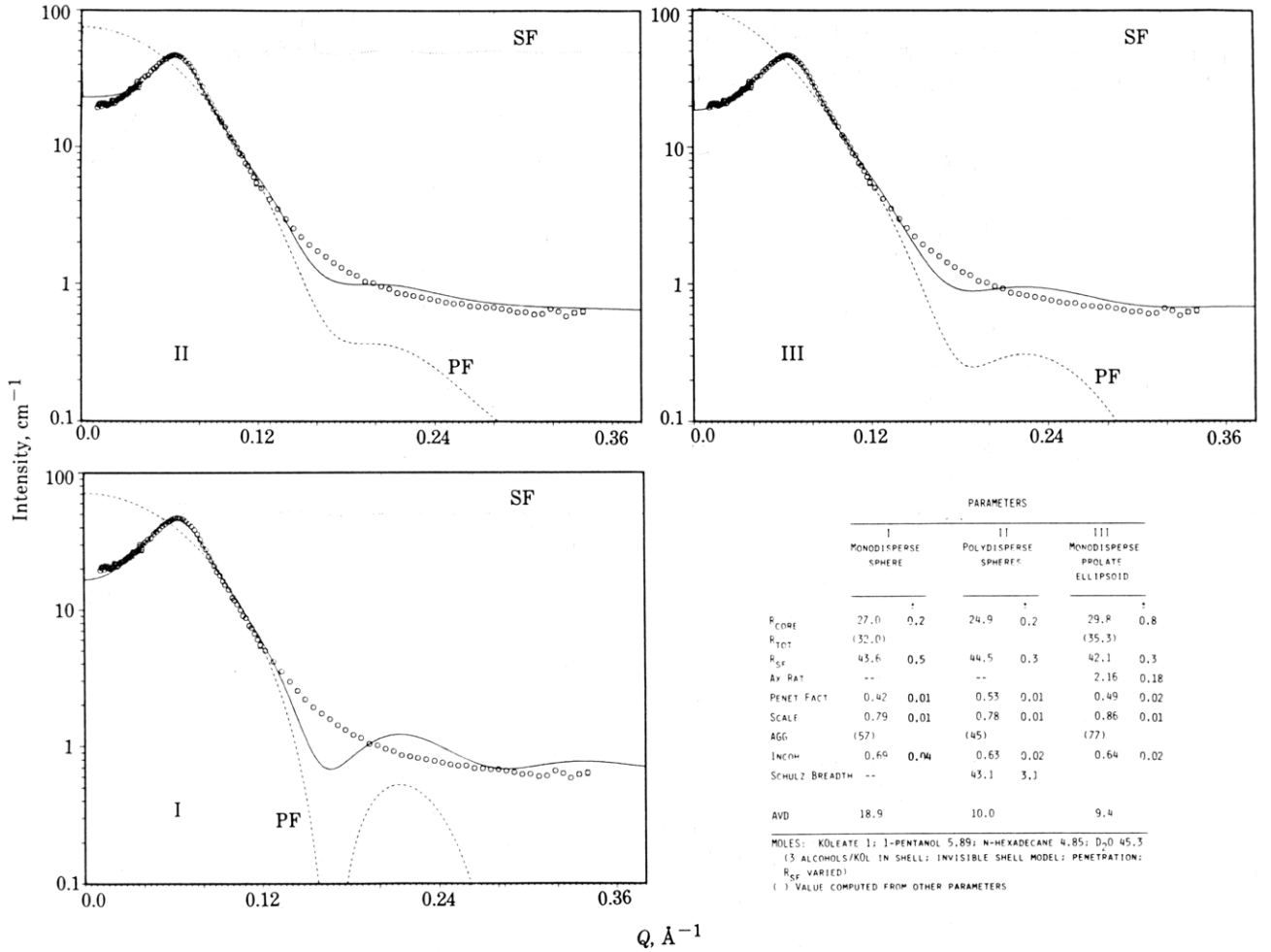

Figure 5. Test of other aggregate geometries; invisible shell model. Composition E.

Table III. Parameters from Least-Squares Fits to Scattering Patterns from Water/Oil Microemulsions of Different Compositions (Monodisperse Oblate Ellipsoid, Invisible Shell Model)

	A[b]	B[b]	C[c]	D[b]	E[b]
mol/mol of KO					
1-pentanol	6	6		6	6
1-hexanol			5.2		
hexadecane	5.5	5.5	5.5	5.5	4.8
D_2O	18	45	45	57	45
parameters					
R_{core}, Å	18.2 ± 0.1	32.7 ± 0.1	37.9 ± 0.2	37.1 ± 0.1	28.2 ± 0.1
R_{tot}, particle[a]	(25.0)	(38.9)	(45.1)	(42.8)	(33.4)
R_{sf}, struct function	26.1 ± 0.1	44.2 ± 0.1	49.8 ± 0.2	52.5 ± 0.3	42.0 ± 0.1
axial ratio	0.46 ± 0.01	0.47 ± 0.01	0.50 ± 0.01	0.47 ± 0.01	0.51 ± 0.00
penet fact	0.43 ± 0.01	0.45 ± 0.00	0.63 ± 0.01	0.44 ± 0.01	0.46 ± 0.00
scale	0.89 ± 0.01	0.98 ± 0.00	1.11 ± 0.01	0.96 ± 0.02	0.87 ± 0.00
AGG[a]	(42)	(104)	(163)	(120)	(65)
incoherent	0.09 ± 0.01	0.27 ± 0.01	0.36 ± 0.02	0.24 ± 0.01	0.59 ± 0.01
AVD	1.2	3.0	5.3	6.3	3.0

[a] Computed from other parameters. [b] Computations for 3 mol of alcohol/mol of KOl in particle. [c] Computations for 2.5 mol of alcohol/mol of KOl in particle.

Table III). Once occurrence of aggregation at all compositions is accepted, variations in core radius are not surprising. Core radius and aggregation increase as water/amphiphile increases, for constant amphiphile/hydrocarbon ratios (A, B, D). Not quite as expected for increase in disperse phase/hydrocarbon ratios, at constant water/amphiphile, is the decrease in aggregate size (B vs. E); possibly the distribution of alcohol in the aggregates is greater in this case. Although the molar concentrations are not quite the same, it appears that substitution of hexanol for pentanol increases aggregate size (B vs. C). Axial ratios are similar for the different concentrations, about 0.5.

Conclusions

The scattering patterns establish, without recourse to models, that structures characterized by dimensions of a few tens of angstroms are present in these solutions. In our attempts to find a model consistent with all results, we found that account had to be taken for penetration of

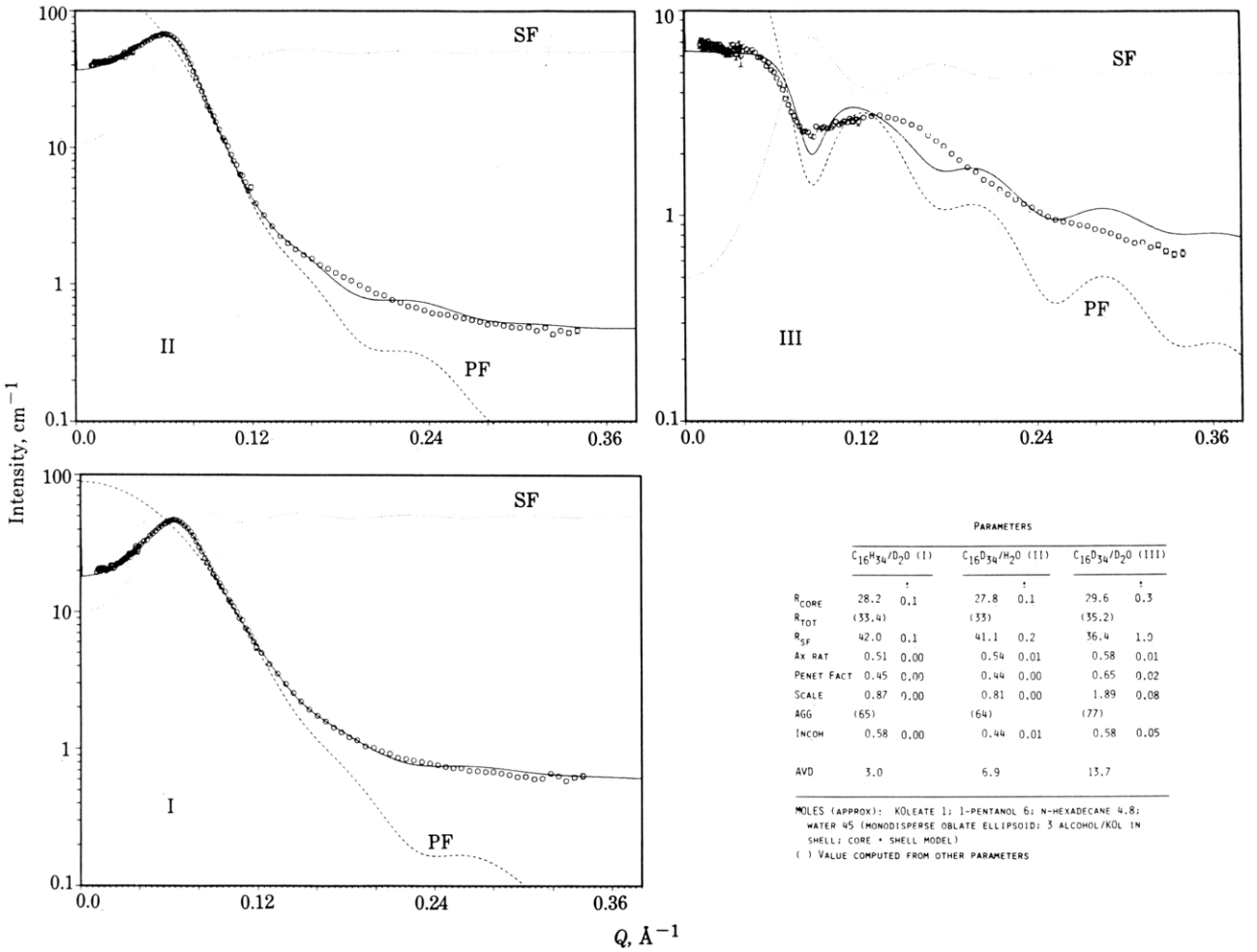

PARAMETERS

	$C_{16}H_{34}/D_2O$ (I)	±	$C_{16}D_{34}/H_2O$ (II)	±	$C_{16}D_{34}/D_2O$ (III)	±
R_{CORE}	28.2	0.1	27.8	0.1	29.6	0.3
R_{TOT}	(33.4)		(33)		(35.2)	
R_{SF}	42.0	0.1	41.1	0.2	36.4	1.0
Ax rat	0.51	0.00	0.54	0.01	0.58	0.01
Penet Fact	0.45	0.00	0.44	0.00	0.65	0.02
Scale	0.87	0.00	0.81	0.00	1.89	0.08
Agg	(65)		(64)		(77)	
Incoh	0.58	0.00	0.44	0.01	0.58	0.05
AVD	3.0		6.9		13.7	

MOLES (APPROX): KOLEATE 1; 1-PENTANOL 6; N-HEXADECANE 4.8; WATER 45 (MONODISPERSE OBLATE ELLIPSOID; 3 ALCOHOL/KOL IN SHELL; CORE + SHELL MODEL)
( ) VALUE COMPUTED FROM OTHER PARAMETERS

Figure 6. Fits to systems of different contrasts; core plus shell model.

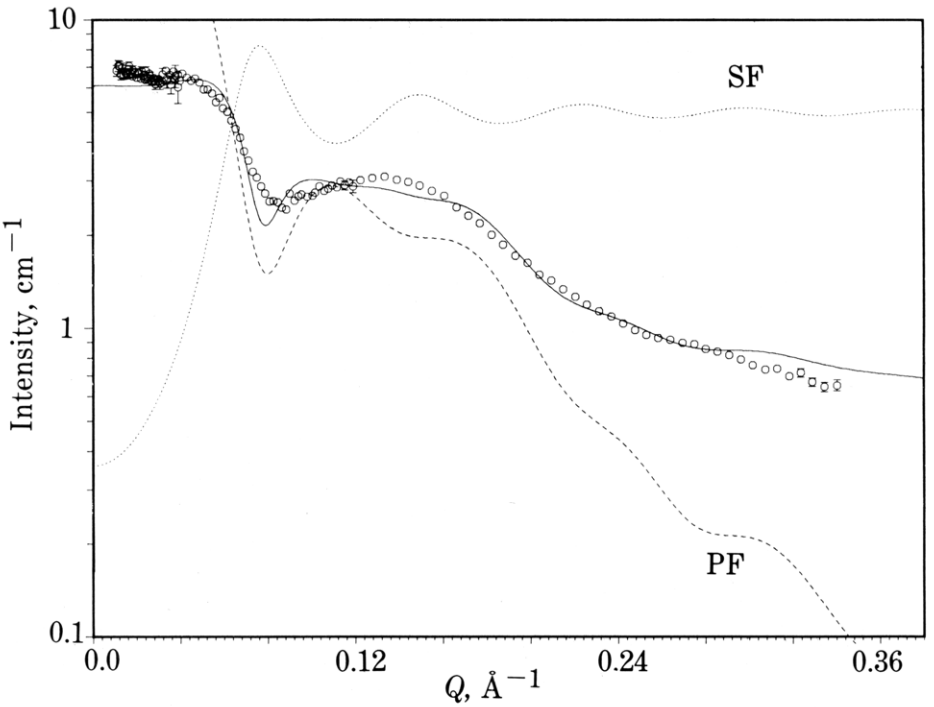

Figure 7. Core + penetrated shell fit to composition G (D_2O and $C_{16}D_{34}$). Alcohols/potassium oleate in aggregate varied, 5.1 ± 1.9. Other varied parameters: R_{core} = 27.4 ± 1.1 Å; shell thickness, 14.0 ● 1.3; ax. rat., 0.35 ± 0.2; penetration fact., 0.38 ± 0.04; scale, 1.5 ± 0.3; incoh, 0.68 ± 0.04. Derived parameters: agg, 60; $R_{tot} = R_{sf}$, 43. AVD = 7.1

the aggregation shell by solvent or the shells of other particles. In trying to define the geometries of the aggregates, we have used the simplest arrangement possible to describe the dominant contrast. We find that reasonably good fits could be obtained for all systems on the assumption of monodisperse oblate ellipsoids, and param-

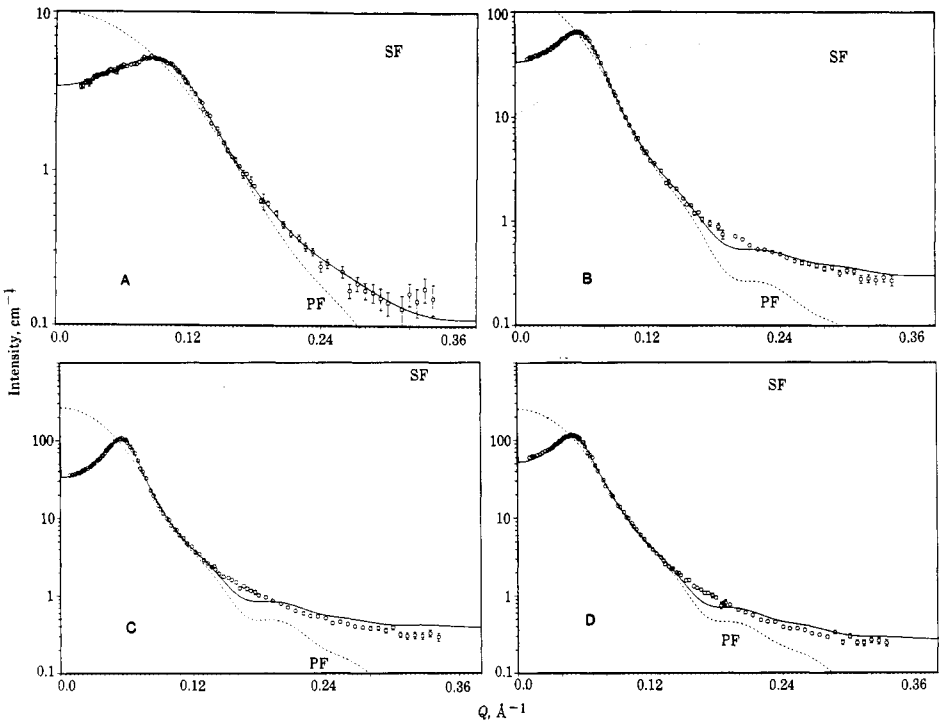

Figure 8. Fits to various compositions; invisible shell model; parameters in Table III.

eters were consistent for compositions essentially the same except for labeled components.

The fits for other geometries or distributions were substantially worse, monodisperse spheres being definitely excluded and polydisperse spheres and monodisperse prolate ellipsoids providing inferior agreement. In view of the uncertainties in the computation of structure functions for polydisperse systems and for anisotropic particles (eq 2), one should be cautious in concluding that the particles are in fact oblate ellipsoids. It is further probable that a one-shell model oversimplifies the actual situation; it is plausible that there is a relatively tight shell around the core, along the lines suggested in ref 22, with a penetrated shell outside. With the core radii we obtain, however, the thickness of the inner shell appears to be substantially less than the extended length of the alcohol hydrocarbon; otherwise its volume would be unreasonably large. In any case, our present measurements are insufficient to define unambiguously the parameters for a two-shell model.

The uncertainties in structure functions introduce other ambiguities in the interpretation. It is conceivable that the variation in volume fraction we found empirically necessary for satisfactory fits compensates for errors introduced by using the structure function for a sphere of equivalent volume. Interpenetration of shells is not inherently implausible, however. In this context, the question of why ellipsoidal structures should occur is of interest. With oil-in-water micelles, the extended length of the surfactant chain provides a rational limit to one dimension and implies anisotropy when the aggregate exceeds a certain size. With a core comprised primarily of small species such as water, ellipsoids cannot be explained in this way. One possibility is competition for surface of the core by amphiphiles which would favor configurations of larger surface/volume ratio. If the ratio were increased by change of shape, one would expect higher axial ratios when water/amphiphile ratios are less. However, distribution in smaller particles would also increase surface/volume ratios and the trends of A, B, and D in Table III are more consistent with this explanation. Permeability of spheres possibly might introduce features in the patterns mimicked by equations for ellipsoids, or, conceivably, our fits empirically represent a bicontinuous arrangement in which water is constrained to similar dimensions. We cannot at present choose between these or other possibilities.

The system investigated in ref 23b was similar in components to composition C, different only in that the hydrocarbon was dodecane rather than hexadecane. The volume ratio of water to potassium oleate was, however, 1.44, rather than 2.5 for C. The authors chose to take account of departure from monodisperse spheres by invoking polydispersity, rather than anisotropy. The core radii they report, about 30 Å, are in the range we found and, as one would expect from the trend with water/surfactant ratio in the pentanol microemulsions, are smaller than that of C.

A much broader survey of the single-phase water-in-oil region of these systems is clearly of interest. A surprising aspect of the rather limited part of the single-phase region reported here is the lack of obvious correlation between microscopic structure and the strange electrochemical behavior reported in the literature reviewed earlier. We see nothing so far to explain the profound reported differences in properties between systems containing pentanol and hexanol.

Acknowledgment. We are grateful to Dr. Roberto Triolo for many discussions and helpful guidance. Work at the University of Tennessee was sponsored by the National Science Foundation (CHE-8308362). Small-angle neutron measurements were carried out at the National Center for Small-Angle Scattering Research (NCSASR). The NCSASR is funded by National Science Foundation Grant DMR-77-244-58 through Interagency Agreement 40-637-77 with the Department of Energy (DOE) and is operated by the U.S. Department of Energy under Contract DE-AC05-840R21400 with the Martin Marietta Energy Systems, Inc. One of the authors (E.C.) acknowledges supplemental support from the "Progetto Chimica Fine e Secondaria" of CNR (Rome).